

## Research Article

# Generation of OAM Radio Waves Using Circular Vivaldi Antenna Array

**Changjiang Deng, Wenhua Chen, Zhijun Zhang, Yue Li, and Zhenghe Feng**

*State Key Laboratory of Microwave and Digital Communication, Tsinghua University, Beijing 100084, China*

Correspondence should be addressed to Changjiang Deng; [dengcj11@gmail.com](mailto:dengcj11@gmail.com)

Received 5 March 2013; Accepted 10 April 2013

Academic Editor: Yuan Yao

Copyright © 2013 Changjiang Deng et al. This is an open access article distributed under the Creative Commons Attribution License, which permits unrestricted use, distribution, and reproduction in any medium, provided the original work is properly cited.

This paper gives a feasible and simple solution of generating OAM-carrying radio beams. Eight Vivaldi antenna elements connect sequentially and fold into a hollow cylinder. The circular Vivaldi antenna array is fed with unit amplitude but with a successive phase difference from element to element. By changing the phase difference at the steps of  $0, \pm 45^\circ, \pm 90^\circ, \pm 135^\circ$ , and  $180^\circ$ , the OAM radio beam can be generated with mode numbers  $0, \pm 1, \pm 2, \pm 3$ , and  $4$ . Simulations show that the OAM states of  $\pm 2$  and  $\pm 3$  are the same as the traditional states, while the OAM states of  $0, \pm 1$ , and  $4$  differ at the boresight. This phenomenon can be explained by the radiation pattern difference between Vivaldi antenna and tripole antenna. A solution of distinguishing OAM states is also proposed. The mode number of OAM can be distinguished with only 2 receivers.

## 1. Introduction

Electromagnetic (EM) fields can carry not only energy but also angular momentum [1]. The angular momentum is composed of spin angular momentum (SAM) and orbital angular momentum (OAM) describing its polarization state and the phase structure distribution, respectively [2]. SAM, predicted by Poynting in 1909 [3] and experimentally demonstrated by Beth in 1936 [4], has been widely used as the form of circular polarization. However, the research on OAM is not attractive until Allen et al. investigated the mechanism of OAM in 1992 [5]. Henceforth, more and more attention has been paid to OAM in both optical and radio domains.

In contrast to SAM, which has only two possible states of left-handed and right-handed circular polarizations, the theoretical states of OAM are unlimited owing to its unique characteristics of spiral flow of electromagnetic energy and helical wavefront [6]. Therefore, OAM has the potential to tremendously increase the spectral efficiency and capacity of communication systems. Numerous experiments on OAM, originally in optical frequency and then in radio frequency, have been carried out. For instance, the capacity of optical communication systems is largely extended by encoding

information as OAM states or using OAM beams as information carriers for multiplexing [7–10]. In 2007, Thide et al. numerically simulated that OAM beams can also be generated in radio frequency with the help of vector antenna arrays [11]. In 2012, they experimentally demonstrated that two radio waves encoded in different OAM states on the same frequency band can be decoded in the far field for the first time [12]. In [13], Edfos and Johansson compared the technique of using OAM states of radio waves with traditional multiple-in multiple-out (MIMO) communication methods. Simulations showed that, for certain array configurations in free space, traditional MIMO theory leads to eigenmodes identical to the OAM states. Based on this result, they concluded that communicating over the subchannels given by OAM states is a subset of the solutions offered by MIMO.

Compared to MIMO, the concept of OAM in radio frequency is relatively novel, and more research on theory and practice still needs to be developed. The generating of OAM is one of the most important issues. Circular antenna array is the typical structure to generate OAM. In [13, 14], tri-dipole antenna is adopted as array element. The elements are fed by the same signal, but with a successive phase delay from element to element such that after a full turn the phase

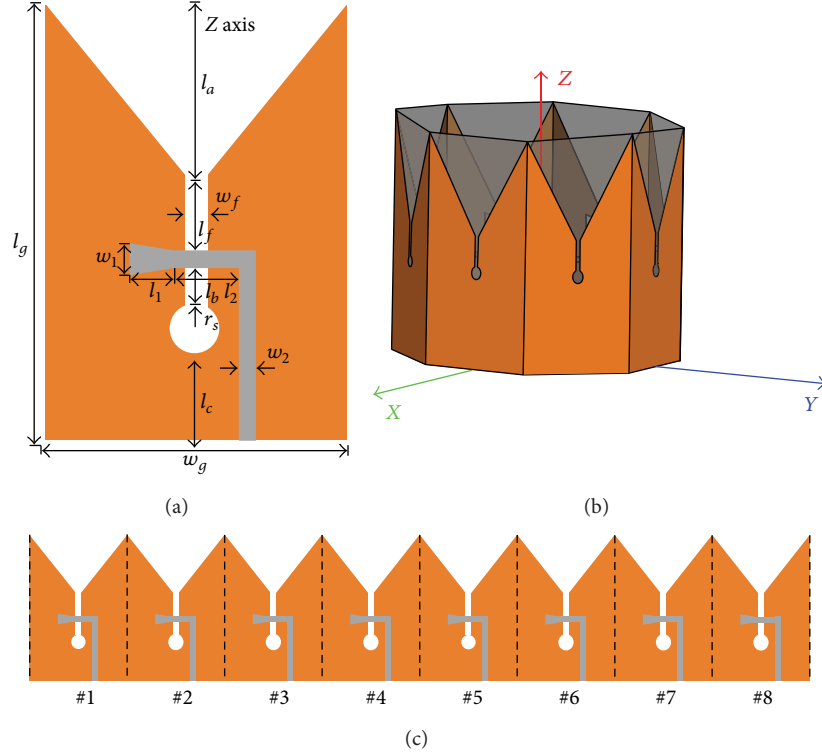


FIGURE 1: Geometry of the proposed antenna: (a) Vivaldi antenna element; (b) Vivaldi circular antenna array; (c) the unfolded view of the antenna array.

TABLE 1: Detailed dimensions (unit: mm).

$l_1$	3.75
$w_1$	3.6
$l_2$	4.25
$w_2$	1.6
$l_f$	7
$w_f$	0.4
$l_g$	60
$w_g$	30
$l_a$	30
$l_b$	16
$l_c$	1.4
$r_s$	2
$r_{out}$	40
$r_{in}$	39.2

has been incremented by an integer multiple  $k$  of  $2\pi$ . In [15], time switched mechanism is introduced. The elements of the circular array are excited with unit amplitude and uniform phase but are energized sequentially such that each element is only switched on for a time period. In this paper, we adopt the same feed method in [14]. Vivaldi antenna is used as the element of circular array and analyzed in detail. Simulations show that the proposed antenna array is a simple and promising candidate to generate OAM.

## 2. Antenna Configuration and Mechanism

Figure 1 shows the geometry of the proposed antenna. The dimensions of the Vivaldi antenna element are depicted in Figure 1(a). A slotted ground and a  $50\ \Omega$  open-ended stub are arranged on the front and back of a FR4 substrate, with relative permittivity  $\epsilon_r = 4.0$  and  $\tan \delta = 0.02$ . The circular antenna array is shown in Figure 1(b), and the planar view of the proposed array is shown in Figure 1(c). Eight Vivaldi antenna elements connect sequentially and fold at an angle of  $45^\circ$  to form a hollow cylinder. The outside radius and inside radius of the cylinder are  $r_{out}$  and  $r_{in}$ , respectively. The thickness  $h$  of FR4 substrate and the width  $w_g$  of ground can be concluded from  $r_{out}$  and  $r_{in}$  according to (1). The detailed values of each parameter are listed in Table 1. Similarly, the circular antenna array can easily be extended into 16 elements or more. Consider

$$h = (r_{out} - r_{in}) \times \cos\left(\frac{360^\circ}{8} \times \frac{1}{2}\right), \quad (1)$$

$$w_g = 2 \times (r_{out} - r_{in}) \times \sin\left(\frac{360^\circ}{8} \times \frac{1}{2}\right).$$

In [14], the generation of OAM radio beams with circular antenna array is deduced in theory. According to the analysis in [14], the  $N$  equidistant elements in the circular antenna array are fed with unit amplitude, but with a successive phase delay from element to element such that after a full turn the phase has been incremented periodically. An OAM-carrying

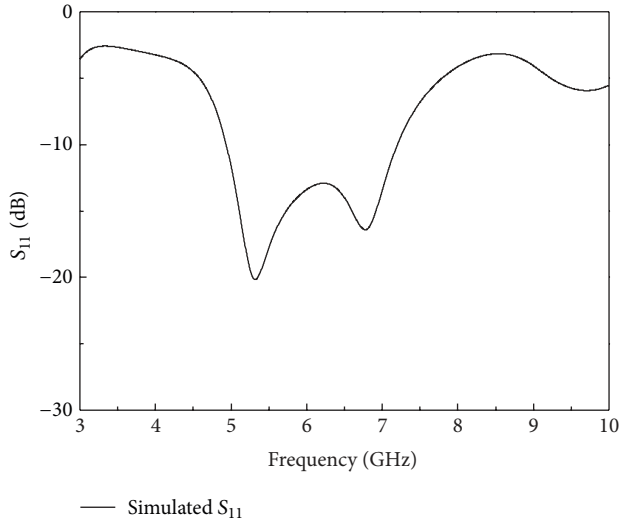


FIGURE 2: Simulated  $S_{11}$  of the proposed Vivaldi element.

radio beam with mode number  $l$  can be generated if the  $n$ th element has phase  $\phi_n = l\varphi_n$ , where  $\varphi_n = 2\pi n/N$  is the angle of the element position. In this paper, we assume that  $N = 8$ . Therefore, the possible OAM states are 0,  $\pm 1$ ,  $\pm 2$ ,  $\pm 3$ , and 4.

### 3. Simulation Results

The antenna was designed and simulated using Ansoft HFSS full-wave simulator based on the finite element method (FEM), according to the parameters listed in Table 1. The operating frequency is designed at 6 GHz. Figure 2 shows the simulated reflection coefficient of the Vivaldi antenna element. The 10 dB reflection coefficient bandwidth is larger than 30%. Owing to the fact that the bandwidth of Vivaldi antenna is wide and the bandwidth is not important in OAM discussion, parameters are not well optimized. Figure 3 shows the simulated gain of the Vivaldi element. It is shown that the pattern of Vivaldi element is broadside. The gain is also high (larger than 7 dB). The characteristics of Vivaldi antenna show that it is a promising candidate to form a uniform circular antenna array.

Figure 4 shows the simulated reflection coefficient of the circular Vivaldi antenna array. Compared with the  $S_{11}$  in Figure 2, the  $S_{11}$  of circular array is better. This improvement can be explained that the ground of array is connected together and larger than the ground of element.

According to the analysis in Section 2, an OAM-carrying radio beam with mode numbers  $l = 0, \pm 1, \pm 2, \pm 3$ , and 4 can be generated if the successive phase difference from element to element is at steps  $0, \pm 45^\circ, \pm 90^\circ, \pm 135^\circ$ , and  $180^\circ$ . The simulations validate the prediction and are shown in Figures 5, 6, and 7.

Figures 5, 6, and 7 show the OAM-carrying radio beams and radiation patterns with all possible mode numbers  $l$ . The concerned area, where the vector and magnitude of electric field are plotted, is placed above the circular array and perpendicular to  $z$ -axis. The size of the concerned area

TABLE 2: Distinguishing rules.

Phase delay	$n$	Judgment: $l$
B after A	2	+1
A after B	2	-1
B after A	4	+2
A after B	4	-2
B after A	6	+3
A after B	6	-3

$l = 0$  and 4 cannot be judged in this condition.

is  $80 \times 80$  mm, and the distance between the antenna array and concerned area is 40 mm.

It is observed that the OAM states of  $\pm 1, \pm 2$ , and  $\pm 3$  are legible when calculating the number of helical wavefronts ( $n$ ) in clockwise direction or anticlockwise direction. Compared with the traditional OAM states, the proposed OAM states of  $\pm 1$  are different along the  $z$ -axis. This difference is due to element. As the traditional element is tripole antenna, the radiation pattern is omnidirectional and the mutual coupling is small. The proposed Vivaldi antenna is broadside and the mutual coupling is strong. When the elements are in phase, a null will produce in broadside, as shown in Figure 5. When the phase difference and the space position between elements coincide, namely,  $\pm 45^\circ$  case, strong directivity will produce in broadside, as shown in Figure 6. It is also observed that the null area at the center is enlarged, when the OAM states increase from  $\pm 1$  to  $\pm 3$ . This phenomenon is also shown in Figure 8, where the directivity varies with different numbers  $l$ . Therefore, the receiving radius vertical to  $z$ -axis should be properly selected to ensure that the receiving position will not be in the null zone of possible OAM states.

Figure 9 illustrates the sketch of OAM generation and reception, where the purple dots indicate antenna element positions and the red dots indicate receiver positions. Two adjacent receivers A and B are adopted in order to distinguish the number of helical wavefront whip ( $n$ ) and the rotated direction of helical wavefront. The rule of judgment is explained in Table 2.

### 4. Conclusion

This paper gives a feasible solution of generating OAM-carrying radio beams. To the authors' knowledge, it is the first time to adopt Vivaldi antenna to provide OAM states. By connecting 8 Vivaldi antenna elements sequentially and folding them into a hollow cylinder, a circular Vivaldi antenna array is configured. Simulations show that the OAM radio beam is generated with mode numbers 0,  $\pm 1, \pm 2, \pm 3$ , and 4, when the elements are fed with unit amplitude and successive phase delays of  $0, \pm 45^\circ, \pm 90^\circ, \pm 135^\circ$ , and  $180^\circ$  from element to element. The differences between traditional OAM states and the proposed OAM states at boresight can be explained by the radiation pattern differences between Vivaldi antenna and tripole antenna. A solution of distinguishing OAM states is also proposed with only 2 adjacent receivers.

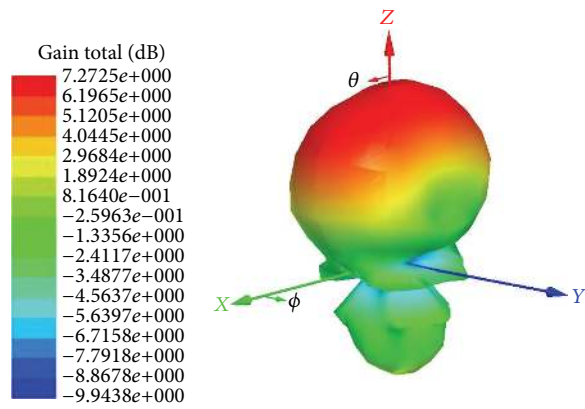


FIGURE 3: Simulated 3D radiation pattern of the Vivaldi element at 6 GHz.

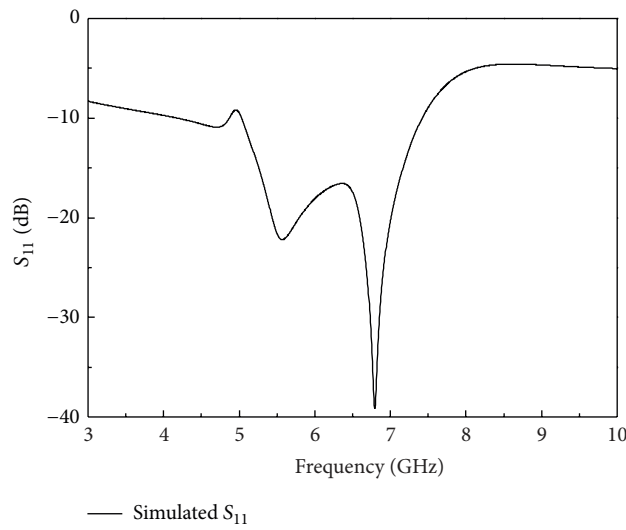


FIGURE 4: Simulated  $S_{11}$  of the proposed Vivaldi circular array.

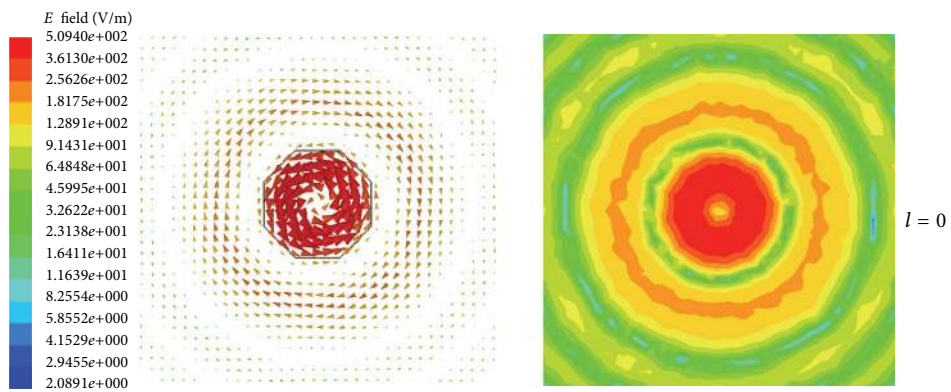


FIGURE 5: The vector and magnitude of electric field with  $l = 0$  at 6 GHz.

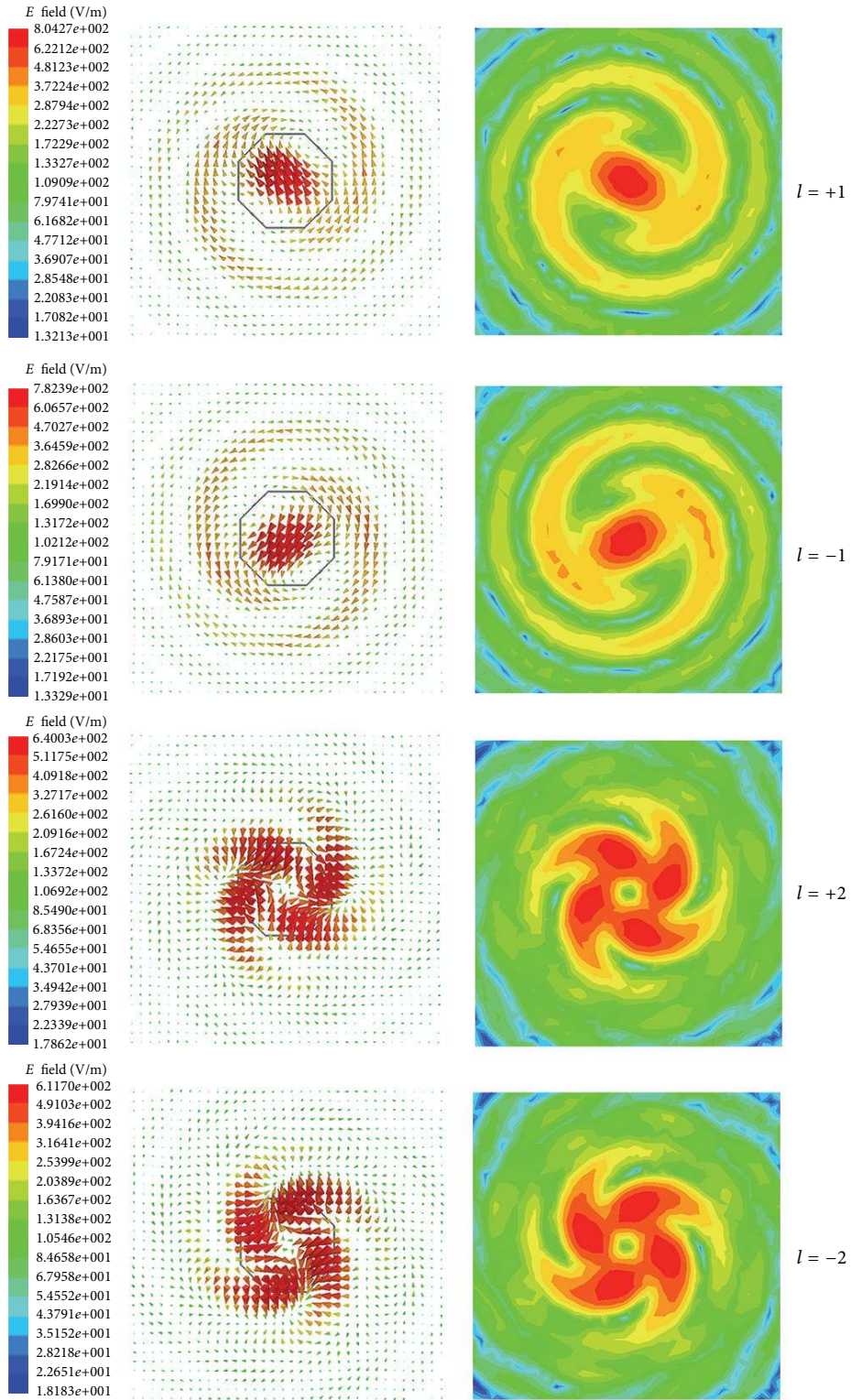


FIGURE 6: The vector and magnitude of electric field with different OAM states at 6 GHz.

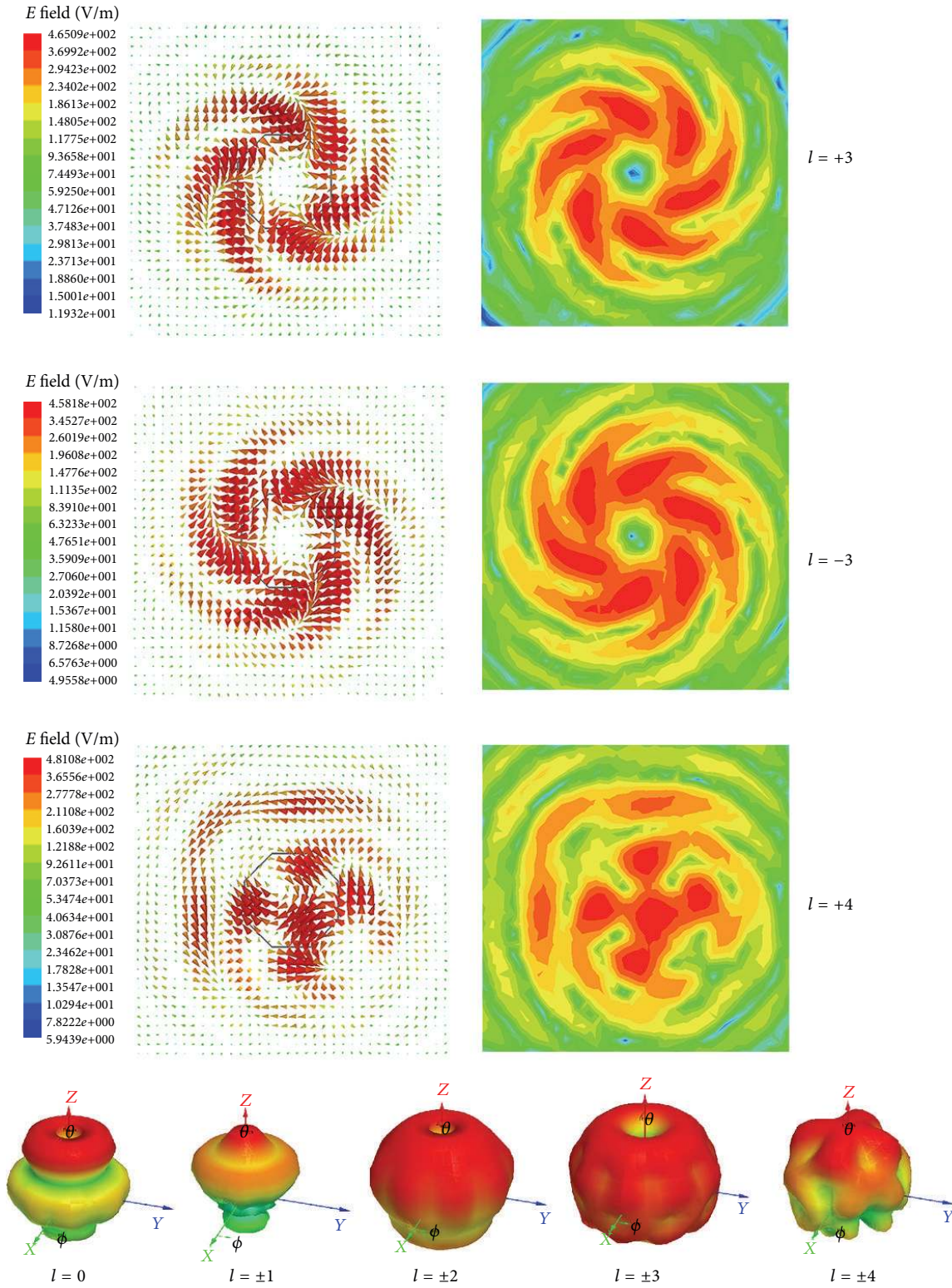


FIGURE 7: The vector and magnitude of electric field and 3D radiation patterns with different OAM states at 6 GHz.

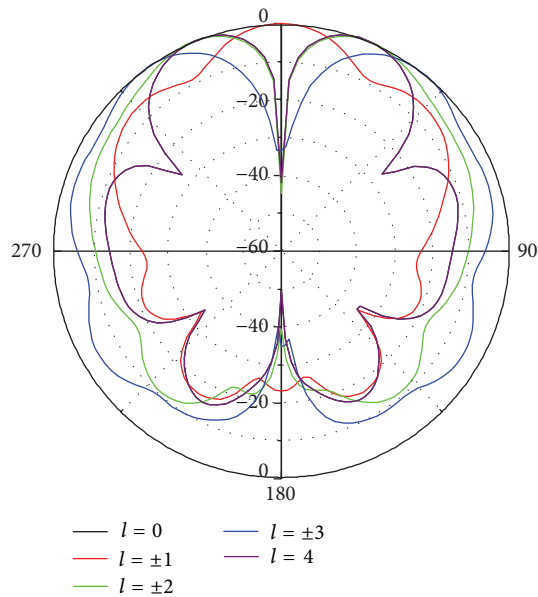


FIGURE 8: Normalized radiation patterns of the circular array with different OAM states in  $xz$ -plane at 6 GHz.

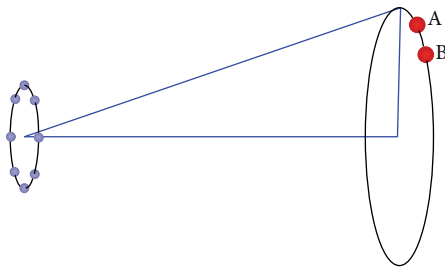


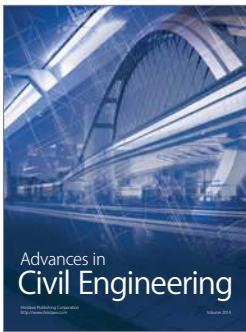
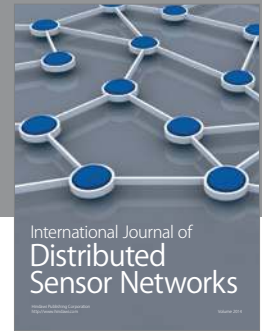
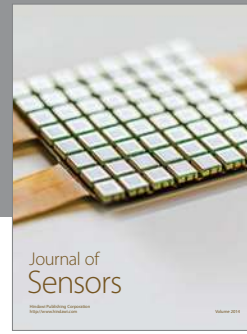
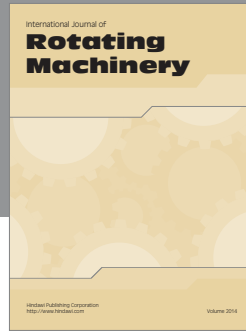
FIGURE 9: Sketch of OAM generation and reception.

## Acknowledgments

This work is supported by the National Basic Research Program of China under Contract 2013CB329002, in part by the National High Technology Research and Development Program of China (863 Program) under Contract 2011AA010202, and the National Science and Technology Major Project of the Ministry of Science and Technology of China 2013ZX03003008-002.

## References

- [1] J. Schwinger, L. L. DeRaad, K. A. Milton, and W. Tsai, *Classical Electrodynamics*, Perseus Books, Reading, Mass, USA, 1998.
- [2] M. K. Ayub, S. Ali, and J. T. Mendonca, "Phonons with orbital angular momentum," *Physics of Plasmas*, vol. 18, no. 10, Article ID 102117, 6 pages, 2011.
- [3] J. H. Poynting, "The wave motion of a revolving shaft, and a suggestion as to the angular momentum in a beam of circularly polarised light," *Proceedings of the Royal Society of London A*, vol. 82, pp. 560–567, 1909.
- [4] R. A. Beth, "Mechanical detection and measurement of the angular momentum of light," *Physical Review*, vol. 50, no. 2, pp. 115–125, 1936.
- [5] L. Allen, M. W. Beijersbergen, R. J. C. Spreeuw, and J. P. Woerdman, "Optical angular momentum of light and the transformation of Laguerre-Gauss laser modes," *Physical Review A*, vol. 45, no. 11, pp. 8185–8189, 1992.
- [6] L. Allen and M. J. Padgett, "Poynting vector in Laguerre-Gaussian beams and the interpretation of their angular momentum density," *Optics Communications*, vol. 184, no. 1, pp. 67–71, 2000.
- [7] J. H. Shapiro, S. Guha, and B. I. Erkmen, "Ultimate channel capacity of free-space optical communications," *Journal of Optical Networking*, vol. 4, pp. 501–516, 2005.
- [8] I. B. Djordjevic, "Deep-space and near-Earth optical communications by coded orbital angular momentum (OAM) modulation," *Optics Express*, vol. 19, no. 15, pp. 14277–14289, 2011.
- [9] Y. Awaji, N. Wada, and Y. Toda, "Demonstration of spatial mode division multiplexing using Laguerre-Gaussian mode beam in telecom-wavelength," in *Proceedings of the IEEE Photonics Conference*, 2010.
- [10] J. Wang, J. Y. Yang, I. M. Fazal et al., "Terabit free-space data transmission employing orbital angular momentum multiplexing," *Nature Photonics*, vol. 6, pp. 488–496, 2012.
- [11] B. Thide, H. Then, J. Sjöholm et al., "Utilization of photon orbital angular momentum in the low frequency radio domain," *Physical Review Letters*, vol. 99, no. 8, Article ID 087701, 5 pages, 2007.
- [12] F. Tamburini, E. Mari, A. Sponselli, B. Thide, A. Bianchini, and F. Romanato, "Encoding many channels on the same frequency through radio vorticity: first experimental test," *New Journal of Physics*, vol. 14, Article ID 033001, 2012.
- [13] O. Edfos and A. J. Johansson, "Is orbital angular momentum (OAM) based radio communication an unexploited area?" *IEEE Transactions on Antennas and Propagation*, vol. 60, no. 2, pp. 1126–1131, 2012.
- [14] S. M. Mohammadi, L. K. S. Daldorff, J. E. S. Bergman et al., "Orbital angular momentum in radio—a system study," *IEEE Transactions on Antennas and Propagation*, vol. 58, no. 2, pp. 565–572, 2010.
- [15] A. Tennant and B. Allen, "Generation of OAM radio waves using circular time-switched array antenna," *Electronics Letters*, vol. 48, no. 21, 2012.



**Hindawi**

Submit your manuscripts at  
<http://www.hindawi.com>

